Peer-reviewed version available at *Atoms* **2019**, *7*, 73; doi:10.3390/atoms7030073

Article

Opacity Corrections for Resonance Silver Lines in Nano-Material Laser-Induced Plasma

Ashraf M. EL Sherbini [1], Tharwat M. EL Sherbini [1], and Christian G. Parigger [2,*]

[1] Laboratory of Laser and New Materials, Faculty of Science, Cairo University, Giza, Egypt; elsherbinia@sci.cu.edu.eg; thelsherbini@hotmail.com

[2] Department of Physics and Astronomy, University of Tennessee/University of Tennessee Space Institute, 411 B. H. Goethert Parkway, Tullahoma, TN – 37388, USA; cparigge@tennessee.edu

* Correspondence: cparigge@tennessee.edu; Tel.: +1-931-841-5690

Abstract: Q-switched laser radiation at wavelengths of 355 nm, 532 nm, and 1064 nm from a Nd: YAG laser was used to generate plasma in laboratory air at the target surface made of compressed nano-silver particles of size 95 ± 10 nm. The emitted resonance spectra from the neutral silver at wavelengths of 327.9 nm and 338.2 nm indicate existence of self-reversal in addition to plasma self-absorption. Both lines were identified in emission spectra at different laser irradiation wavelengths with characteristic dips at the un-shifted central wavelengths. These dips are usually associated with self-reversal. Under similar conditions, plasmas at the corresponding bulk silver target were generated. The recorded emission spectra were compared to those obtained from the nano-material target. The comparisons confirm existence of self-reversal of resonance lines that emerge from plasmas produced at nano-material targets. This work suggests a method for recovery of the spectral line shapes and discusses practical examples. In addition, subsidiary calibration efforts that utilize the Balmer series Hα-line reveal that other Ag I lines at 827.35 nm and 768.7 nm are optically thin under variety of experimental conditions and are well-suited as reference lines for measurement of the laser plasma electron density.

Keywords: laser-induced plasma; atomic spectroscopy; self-reversal; self-absorption; nanoparticles; silver; hydrogen

1. Introduction

Self-absorption as well as self-reversal of radiation from optically thick plasma occur due to processes of re-absorption in the outer-cooler region or in shockwave-induced density variations. The plasma produced by focusing of pulsed laser light on suitable targets suffers from strong inhomogeneity, even when using a well-defined TEM_{00} laser mode[1]. Plasma inhomogeneities lead to strong gradients of plasma parameters (electron density and temperature) from the hot central core to peripheries that is in contact with surrounding air. This cooler plasma peripheries contain large population of atoms in lower atomic states, especially in the ground state. These peripheral atoms are often causing plasma re-absorption[2]. The plasma opacity manifests itself in form of homogeneous absorption of the spectral line that is labelled self-absorption. Effects of self-absorption include an apparent increase of the emitted line full-width at half-maximum (FWHM) and a decrease in spectral line height[3]. Line shape recovery is possible, only if one employs a standard, reliable measure of the true plasma electron density, which is offered by the optically thin Hα- and Hβ- lines[3,4], yet frequently the Hα-line is utilized. For instance, line-of-sight measurements of laser-induced plasma at or near an ice surface[4,5] show self-reversal tips at the un-shifted resonance wavelength of the hydrogen alpha line of the Balmer series. Typical "fingerprints" due to re-absorption include self-reversal and self-absorption[4-11]. In this work, self-absorption and self-reversal parameters, SR and SA, respectively, distinguish between these re-absorption effects.

There are significant challenges when considering self-reversed lines, especially for resonance lines, for the evaluation of the electron density typically measured from the full-width-at-half-maximum, and determination of the temperature that is a function of the spectral radiance. Moreover, spectral line intensities from nano-based materials show differences from the corresponding bulk signals[12]. The theoretical descriptions of self-absorption and self-reversal[5-11] rely on the computation of the emitted radiation when modeling the emitters by a specific distribution.

However, strong enhanced plasma emission was noticed when focusing laser radiation onto targets made of pure nanomaterials[12-14]. This enhanced emission was related to the sudden increase of the population density of the ground state atoms (in the same ratio of amount of enhanced emission $I_{\lambda 0}^{nano}/I_{\lambda 0}^{bulk} \approx N_{\lambda 0}^{nano}/N_{\lambda 0}^{bulk}$ [12-14], i.e., more of cold atoms (N_0^{nano}) exist at the outer peripheries of plasma produced from nanomaterials[14], but without further increase in the plasma excitation temperature[2], . This enhanced emission enables the spectral line intensity $I_{\lambda 0}^{Nano}$ of the resonance lines to exceed the corresponding, upper-limit black body radiation intensity $I_{\lambda 0}^{Nano} \geq B(\lambda_0, T_{ex})$,

$$\mathbf{B}(\boldsymbol{\lambda}_0, \mathbf{T}_{ex}) = \frac{\mathbf{2hc}^2}{\boldsymbol{\lambda}_0^5}\left(\frac{\mathbf{1}}{\exp\{\mathbf{hc}/\boldsymbol{\lambda}_0\mathbf{k_B}\mathbf{T}_{ex}\}-\mathbf{1}}\right), \quad (1)$$

This is because of the relatively local temperature, T_{ex}, in this plasma region. Therefore, and as elaborated by Fujimoto[2], i.e., the measured radiation intensity of the resonance lines are only those that emerge from the outer plasma regions at which the plasma optical depth is unity, hence self-reversal starts to act at the central un-shifted wavelengths of resonance lines that terminate at the ground state. Figure 1 illustrates a homogenized central core, cold periphery, and the emanating "distorted" line shape.

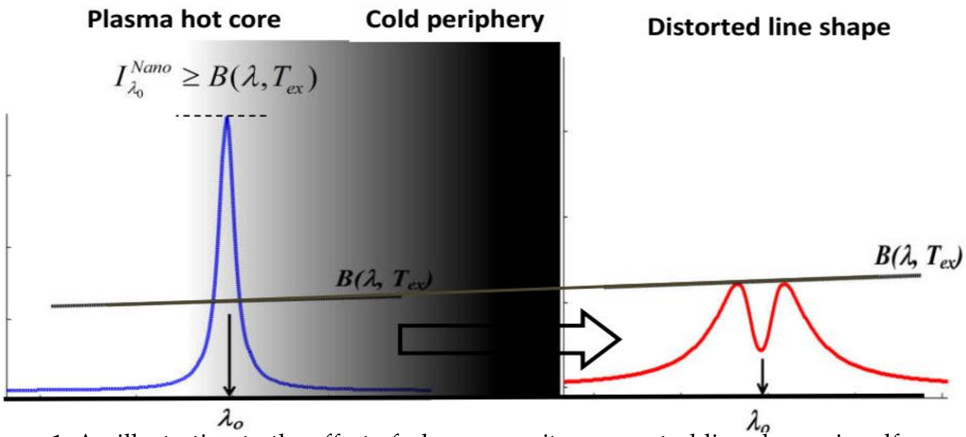

Figure 1. An illustration to the effect of plasma opacity on spectral line shape via self-reversal (red) in comparison to the undistorted shape (blue), together with black body spectral intensity limit (black line) at certain excitation temperature at the plasma outer regions.

There are three effects that modify the line shape: First, the excessive enlargement of line FWHM, second, reduction of spectral radiance imposed by the black body radiation limit and third, the reversed line-shape of the emission line.

This work introduces a method for retrieving the original undistorted shape of self-absorbed lines that are affected simultaneously by self-reversal and self-absorption. The method is based on the availability of certain optically thin spectral lines that originate from upper states of atomic transitions, viz., Ag I lines at 827.35 nm and at 768.7 nm. The method is examined at different laser irradiation wavelengths and at different laser irradiance levels.

 doi:10.20944/preprints201906.0221.v1

Peer-reviewed version available at Atoms 2019, 7, 73; doi:10.3390/atoms7030073

2. Materials and Methods

In the experiments, a Nd:YAG laser device(Quantel model Brilliant B) operates at the fundamental wavelength of 1064 nm and the two harmonics at 352 and 355 nm, with output laser energy per pules of 370 ± 5, 100 ± 4, and 30 ± 3 mJ, respectively. The corresponding spot sizes at the target surface amount to 0.5 ± 0.05, 0.44 ± 0.05, and 0.27 ± 0.03 mm. An optical fiber of 400 mm diameter collects the radiation from the plasma. An echelle type spectrograph (SE200) with an average instrumental bandwidth of 0.2 nm, and an attached intensified charge-coupled device (Andor iStar DH734-18F) acquire the data. The spectral pixel resolution and pixel area amount to 0.02 nm and 196 μm^2, respectively. A xyz-holder allows one to position the optical fiber at distance of 5 mm from the laser-induced plasma.

The time delay and gate width amount to 2 μs for all experiments reported in this work. ICCD KestrelSpec® software subtracts the background stray light contributions. The measured electronic noise level amounts to 20 ± 7 counts across wavelength range of 250 – 850 nm. The measurements of incident laser energy at each laser shot utilize a quartz beam splitter to direct the reflected part (4 %) to a calibrated power-meter (Ophier model 1z02165). A 25 ps fast response photodiode in conjunction with digital storage CRO (type Tektronix model TDS 1012) measures the laser pulse width of 5 ± 1 ns. A set of calibrated neutral density filters adjusts the energy/pulse. The DH2000-CAL lamp (Ocean Optics SN037990037) allowed us to correct for the sensitivity of detection system composed of spectrograph, intensified camera and optical fiber. A 500 kg/cm^2 press prepared the silver nanomaterial powder (from MKNANO®) to produce a less brittle tablet without further purification or heat treatments. The nanoparticle size equals 95 ± 10 nm, as confirmed from measurements with a transverse electron microscope.

4. Results and discussion

An example of the self-reversed resonance lines from the neutral silver atoms is presented in Figure 2 after laser irradiation of different wavelengths, namely, 355 nm, 532 nm and 1064 nm.

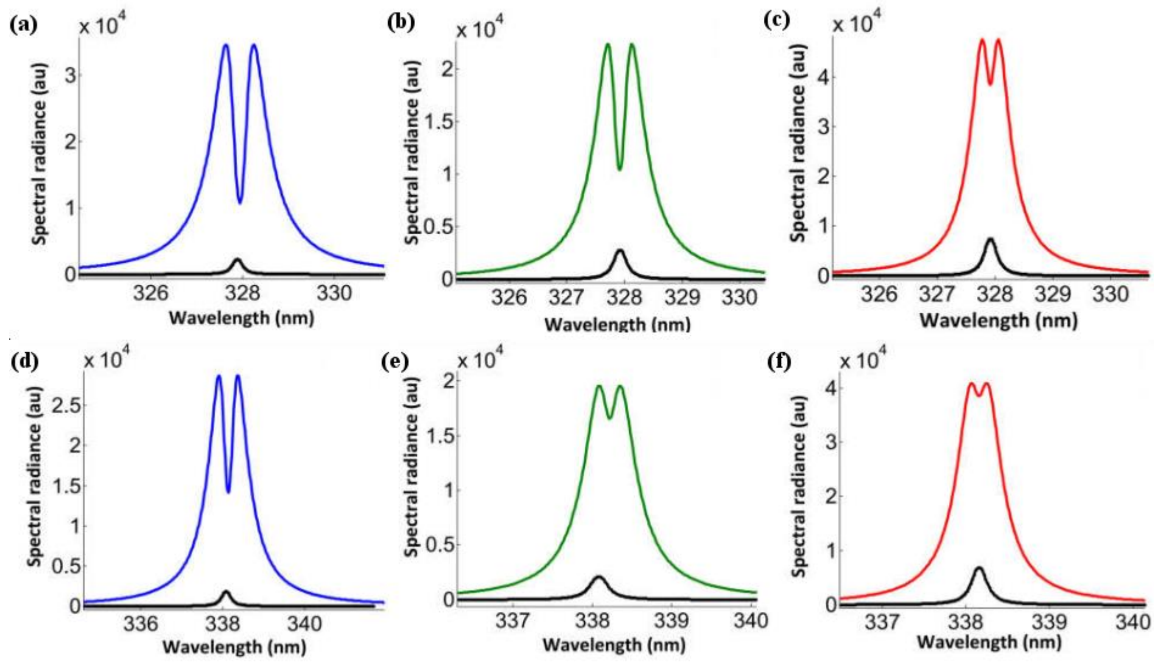

Figure 2. The effect of self-reversal on the resonance Ag I transition from nano-silver plasmas with respect to bulk target (black). Different laser irradiation wavelengths are indicated by different colors: blue for 355 nm, green for 532 nm and red for the 1064 nm.

Preprints (www.preprints.org) | NOT PEER-REVIEWED | Posted: 22 June 2019 doi:10.20944/preprints201906.0221.v1

Peer-reviewed version available at Atoms 2019, 7, 73; doi:10.3390/atoms7030073

In Figure 2, the upper self-reversed spectral lines emerge from plasma generated at the surface of the nano-silver target. The lower black spectra are the corresponding lines for the same transition and under the same experimental conditions but from the bulk-silver target. One can notice significantly more self-absorption of the plasma from nano-silver than for plasma from bulk-silver.

For the resonance transitions of the Ag I lines at 327.9 and 338.2 nm, Figures 3 to 5 illustrate recorded and fitted nano-material silver lines with central dips at line center. The Stark shift is smaller than the instrument width.

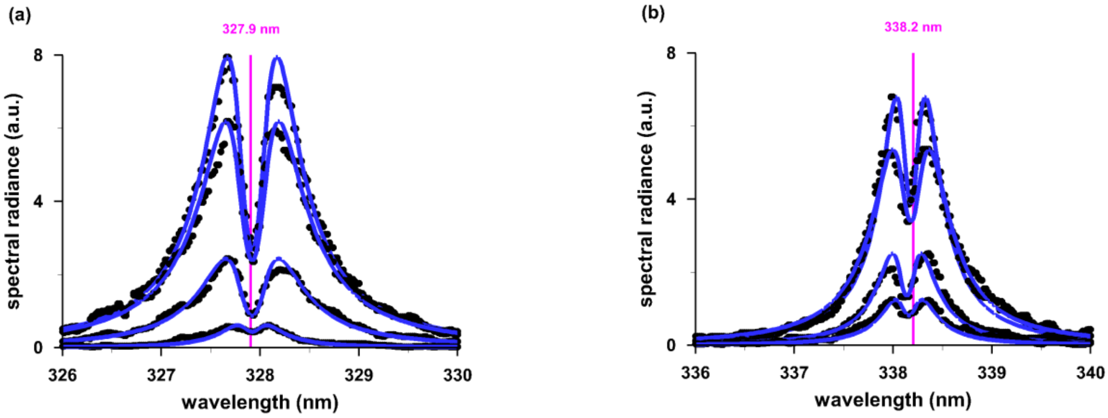

Figure 3. AgI (**a**) 327.9 nm and (**b**) 338.2 nm lines, 355-nm excitation, fluences of 13.5, 9.6, 5 and 2.1 J/cm^2.

The two sets of spectra show the results captured from nano-material silver targets with 355 nm radiation. The self-reversal of plasma radiation from nano-silver material is typically absent in investigations of laser-induced plasma with bulk-silver targets for otherwise similar experimental conditions. Figure 3 shows well-developed spectral dips. Accordingly, Fig. 4 displays recorded

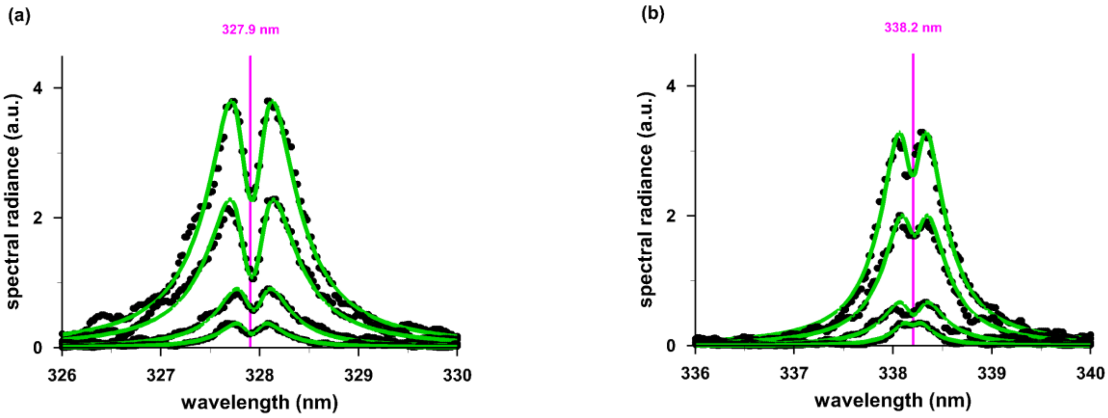

Figure 4. Ag I (**a**) 327.9 nm and (**b**) 338.2 nm lines, 532-nm excitation, fluences of 13.5, 11.5, 8, and 6 J/cm^2.

spectra obtained with 532 nm excitation.

Figure 4 indicates diminished self-absorption when compared to Fig. 3. For 1064 nm laser excitation, Fig. 5 displays even smaller self-absorption phenomena for the two silver lines.

 doi:10.20944/preprints201906.0221.v1

Peer-reviewed version available at Atoms 2019, 7, 73; doi:10.3390/atoms7030073

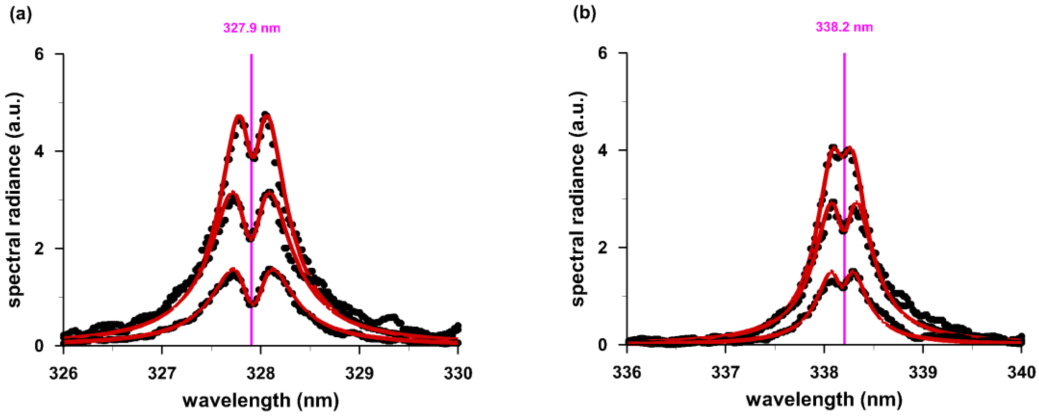

Figure 5. AgI (**a**) 327.9 nm and (**b**) 338.2 nm lines, 1064-nm excitation, fluences of 13.5, 11.5, 8, and 6 J/cm².

In view of Figs. 3 to 5, one can see that it would be challenging to extract the full-width at half-maximum for determination of electron density. It would be required to extract the FWHM of the line after opacity corrections due to self-reversal and self-absorption effects.

The introduced correction procedures are based on precise knowledge of "true" electron density of the nan-material plasma. The reliable H_α line was supposed to provide a measure for electron density[3], but unfortunately, the H_α line is absent when employing green and blue laser beams for plasma generation with nano-silver. Consequently, one needs to identify other suitable optically thin lines.

In the process of locating suitable lines in place of $H\alpha$, an extensive examination of emission spectral lines from the neutral silver discovers that only two Ag I lines at 827.35 nm or at 768.7 nm are suitable candidates for reliable measurement of the 'true' electron density. The inferred electron densities compare nicely with the corresponding values obtained from analysis of the hydrogen alpha line of the Balmer series. Figure 6 illustrates the results, and Table 1 shows the comparisons.

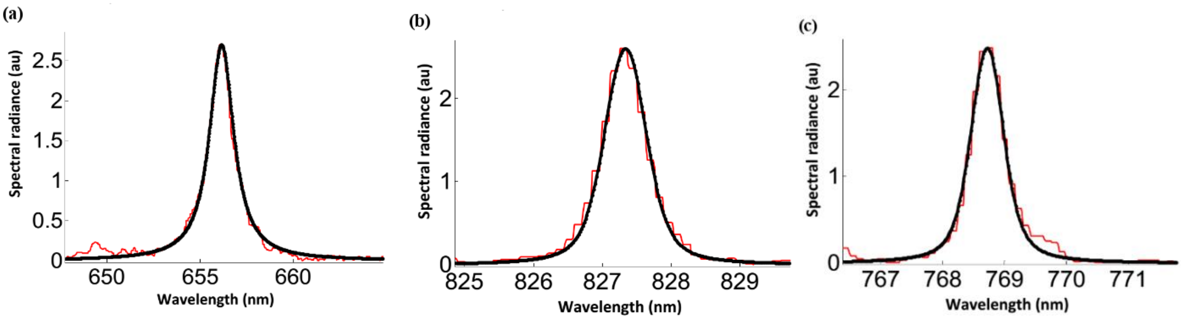

Figure 6. Recorded spectra for (**a**) H_α at 656.28 nm, (**b**) Ag I at 827.35 nm, and (**c**) Ag I at 768.7 nm. Laser fluence 9.6 J/cm², 1064-nm excitation.

Table 1. Electron densities, n_e, in units of $10^{17} cm^{-3}$ for different fluence, 1064-nm excitation.

laser fluence (J/cm²)	n_e: H_α 656.28 nm	n_e: Ag I 827.35 nm	n_e: Ag I 768.7 nm
9.94	1.64	1.66	1.76
7.46	0.76	0.77	0.76
5.9	0.63	0.66	0.70
4.47	0.57	0.55	0.58

Preprints (www.preprints.org) | NOT PEER-REVIEWED | Posted: 22 June 2019 doi:10.20944/preprints201906.0221.v1

Peer-reviewed version available at Atoms 2019, 7, 73; doi:10.3390/atoms7030073

There is excellent agreement of the measured electron density from the H_α and the two optically thin silver lines. The two silver lines Ag I at 827.35 nm and at 768.7 nm are suitable for electron density determination in nano- and bulk- material for the following reasons: First, the Ag lines emerge from the upper states *4d^10^6s-4d^10^5p* with almost empty lower and highly excited state *4d^10^6s* that minimizes the possibility of plasma re-absorption by highly populated low atomic states. Second, both lines are observed in emission spectra of neutral silver under nearly all conditions.

The experimental evaluation included change of the incident laser fluence in the range from 5 to 10 J/cm² and measurement of the emission spectra during IR laser irradiation. The lines are Voigt-fitted to recorded spectral radiances as indicated by the solid black lines in Figure 6. The Stark broadening parameters for both lines are archived in Stark tables[15]: At the reference electron density of $N_e^{ref} = 10^{17}$ cm^{-3}, the Stark broadening parameter, ω_S^{AgI}, amounts to ω_S^{AgI} = 0.18 ± 0.06 nm.. The Lorentzian components of the emitted lines, λ_S^{AgI}, were extracted. The electron densities listed in Table 1 were evaluated with the help of the expression, $n_e^{AgI} \approx N_e^{ref} (\lambda_S^{AgI} / \omega_S^{AgI})$, and then compared with the corresponding values obtained from Hα.

For analysis of the self-absorbed spectra in Figure 2, notice line reversal at the center wavelength, λ_0, and weaker effects in the wings that lead to distortions. The transmittance [3,6], $T(\tau_{\lambda_0})$, is related to the escape factor [3,6] and it depends on the optical thickness of the plasma, τ_{λ_0}.

The transmittance, $T(\tau_{\lambda_0})$, is modeled with a Lorentzian spectral line shape, $\varphi(\lambda)$,

$$T(\tau_{\lambda_0}) = \int \varphi(\lambda) e^{-\tau_{\lambda_0}\varphi(\lambda)/\varphi_0} d\lambda, \qquad \varphi(\lambda) = \frac{1}{\pi}\frac{0.5\,\Delta\lambda_S}{(\lambda-\lambda_0)^2+(0.5\,\Delta\lambda_S)^2}, \tag{2}$$

where $\Delta\lambda_s$ denotes the full-width at half-maximum (FWHM) of the normalized spectral line shape of magnitude φ_0 at line center. The plasma optical thickness at line center, τ_{λ_0},

$$\tau_{\lambda_0} = \int_{-\ell}^{0} \kappa(\lambda_0) d\ell, \tag{3}$$

is defined in terms of integrated absorption coefficient, $\kappa(\lambda)$, of a spectral line measured along the line-of-sight, ℓ, at the transition wavelength, λ_0. Figure 7 illustrates results for τ_{λ_0} ranging from 0.25 to 2 at equal steps of 0.25, and for fixed Lorentzian FWHM of $\Delta\lambda_s$ = 0.5 nm. The line shape indicates a flat top for unity optical thickness, i.e., $\tau_{\lambda_0} = 1$. For values higher than unity,

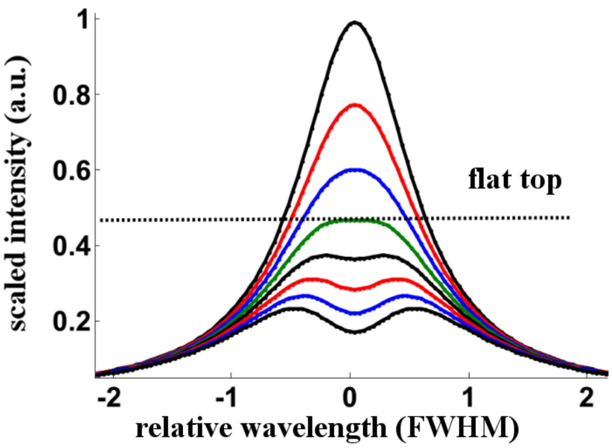

Figure 7. Line shapes $\varphi(\lambda)e^{-\tau_{\lambda_0}\varphi(\lambda)/\varphi_0}$ vs. wavelength, λ, for fixed $\Delta\lambda_s$ = 0.5 nm. Values of τ_{λ_0} range from 0.25 to 2.0 in steps of 0.25.

Preprints (www.preprints.org) | NOT PEER-REVIEWED | Posted: 22 June 2019 doi:10.20944/preprints201906.0221.v1

Peer-reviewed version available at Atoms 2019, 7, 73; doi:10.3390/atoms7030073

self-absorption affects the line shape primarily at the center[2].

The fitting of the argument in Eq. (2) to the experimentally measured line shape can be formulated with two line-shape parameters, namely, the self-absorbed Lorentzian FWHM, $\Delta\lambda_{S1}$, and the optical depth, τ_{λ_0}, at line center.

The self-reversal parameter, SR, is introduced for a quantitative description of the measured line shapes. The parameter SR indicates the ratio of transmitted and of weakly ($\kappa(\lambda)\,\ell \ll 1$) affected intensities at line center,

$$\mathrm{SR} = \frac{1 - e^{-\tau_{\lambda_0}}}{\tau_{\lambda_0}} \leq 1\,, \tag{4}$$

or in terms of the transmittance, $\mathrm{SR} = T(\tau_{\lambda_0})$. Self-reversal diminishes the peak spectral radiance as well. In comparison with self-absorption, self-reversal causes further apparent enlargement of the FWHM, $\Delta\lambda_{S2}$, with $\Delta\lambda_{S2} > \Delta\lambda_{S1}$. In analogy with the derivation of self-absorption[3], one can write $\Delta\lambda_{S2} = \Delta\lambda_{S1}\ \mathrm{SR}^{\alpha}$. The value for the exponent is taken to be $\alpha = -0.54$, in analogy to previously reported self-absorption studies[3]. The self-reversal factor, SR, is functionally identical to that for the self-absorption factor[3], SA, $\Delta\lambda = \Delta\lambda_{S0}\ \mathrm{SA}^{\alpha}$. Here, $\Delta\lambda$ and $\Delta\lambda_{S0}$ indicate the FWHM of spectral lines with and without self-absorption, respectively.

Figure 8 summarizes two typical examples of the discussed spectral line shape analysis for the measured Ag I lines at 327.9 nm and 338.2 nm. Figs. 8 (a) and (d) display self-reversed data, Figs. 8 (b) and (e) portray corrected lines that are still self-absorbed, and Figs. 8 (c) and (f) illustrate the retrieved line-shapes when using data from the optically thin line at 827 nm.

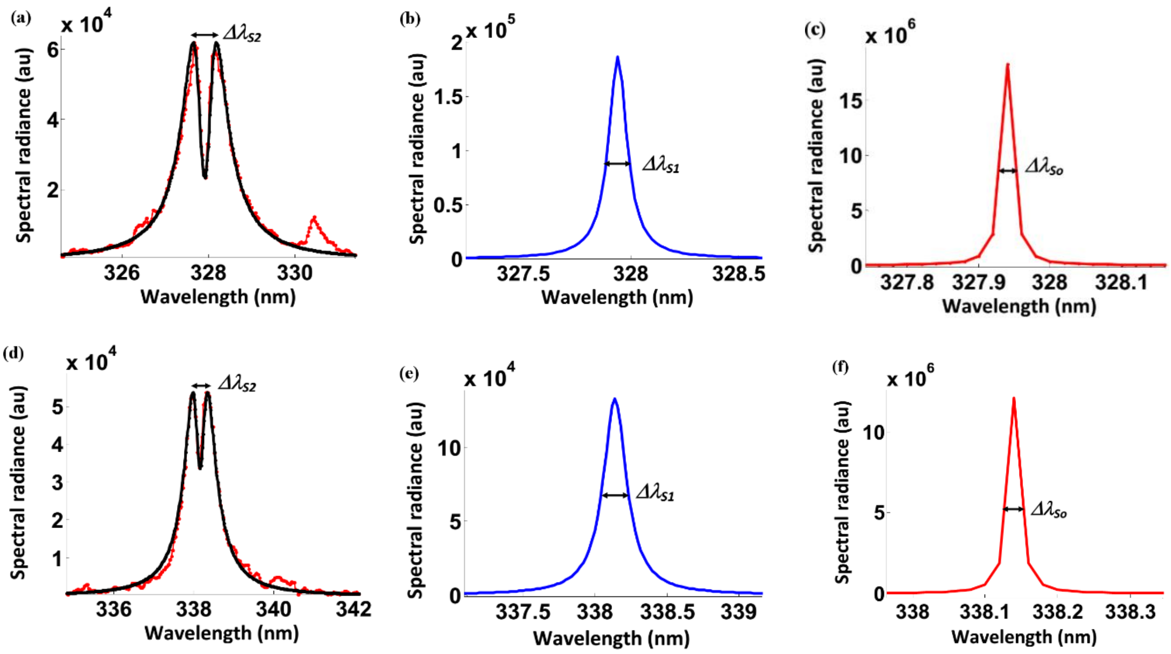

Figure 8. Line shapes (**a**) self-reversed $\Delta\lambda_{S2} = 0.37$ nm, SR = 0.3, $T(\lambda)$ =33 %; (**b**) Self-absorbed $\Delta\lambda_{S1} = 0.2$ nm, $n_{e1} = 4.2 \times 10^{18}$ cm^{-3}, SA = 0.01; (**c**) Reconstructed 327.9-nm optically thin line: $\Delta\lambda_{S0} = 0.017$ nm, $n_{e1} = 3.5 \times 10^{17}$ cm^{-3}, SA = 1. (**d**) $\Delta\lambda_{S2} = 0.32$ nm, SR = 0.38, $T(\lambda)$ =40 %, (**e**) $\Delta\lambda_{S1} = 0.19$ nm, SA = 0.01, and (**f**) 338.2-nm line: $\Delta\lambda_{S0} = 0.017$ nm, $n_{e1} = 3.5 \times 10^{17}$ cm^{-3}, SA = 1. Light pulses for (a) and (d) of fluence 13.5 J/cm^2 at 355 nm generated laser plasma. Reconstruction for (c) and (f) is accomplished with data from the 827-nm line.

Preprints (www.preprints.org) | NOT PEER-REVIEWED | Posted: 22 June 2019 doi:10.20944/preprints201906.0221.v1

Peer-reviewed version available at *Atoms* **2019**, *7*, 73; doi:10.3390/atoms7030073

The measured widths and plasma transmission percentages (typically 33% and 40% for the reported experiments) are included in the figure captions. The theoretical, asymptotic form for the transmittance of a Lorentzian line profile [2,6] equals

$$T_{theory}(\tau_{SR}) \sim 1/\ \sqrt{\pi\, \tau_{SR}}\ . \quad (5)$$

The theoretical transmittances are compatible with SR factors of 0.32 and 0.38. The measured line shapes are well-described by the fitted Lorentzians. However, for sake of simplicity, this discussion omits Gaussian components due to instrumental broadening of $\Delta\lambda_{instrument}$ ~ 0.12 nm. Figs. 8 (a) and (d) show a significant reduction in intensity along with an apparent increase in broadening ($\Delta\lambda_{S2}$). The self-reversal coefficients are relatively small (SR = 0.32 and SR = 0.38), but due to line center effects [2,5-10] dips occur. Noteworthy in this work, self-reversal (quantified by the coefficient SR) is almost independent of the laser fluence, but self-absorption (SA) changes monotonically with laser fluence.

In this example, the self-reversal peak separation provides values for $\Delta\lambda_{S2}$, using the FWHM of lines with the dip would cause even larger discrepancies for the electron density, n_e. From Equation (5), computed $\Delta\lambda_{S1}$ would show electron densities that are ~ ten times higher than obtained from the optically thin line that was retrieved by comparison with 827-nm results. When using lower fluence levels for these two lines, larger variances occur in inferred n_e values. From Eq. (6), a factor of ten higher electron density means that the self-absorption factor is of the order of SA ~ 0.01. For self-absorption, the magnitude of the peak spectral irradiances can be evaluated[3] using $I_0(\lambda_0) \sim I_1(\lambda_0)/SA$, leading to two orders of magnitude higher irradiances. Such discrepancy indicates significant self-absorption and line reversal for the selected example.

5. Conclusions

Self-absorption may lead to a decrease in the peak line intensity up to two orders of magnitude, including appearance of self-revered lines. Even after taking into consideration the line shape effects, occurrence of self-absorption for a measured line contraindicates plasma electron density and temperature measurements from that line. The experimentally measured transmission factors for the 327.9-nm and 338.2-nm lines change with incident laser fluence. The theoretical analysis predicts transmittance values consistent with the measured ones within the experimental margins of error. The optically thin, 827-nm silver line allows one to determine the electron density showing decreases as expected from 3.5×10^{17} to 1.1×10^{16} cm^{-3} with decreasing laser fluence. However, as self-absorption of the silver 338.2 nm line decreases with decreasing fluence, the variations of inferred electron densities are larger than anticipated, or the 338.2 nm line shows a larger standard deviation than the 827 nm line. The Ag I line at 338.2 nm disappears for a laser fluence of 2.1 J/cm^2. Finally, plasma opacity manifests itself as a combination of self-absorption and self-reversal effects, and line recovery would require results from an optically thin line, or in other words, self-absorbed or self-reversed lines are ill-suited as electron density diagnostic of laser plasma.

Author Contributions: Ashraf M. EL Sherbini conceived and performed the experiments. Ashraf M. EL Sherbini the result together with Christian G. Parigger, and all authors contributed to the writing of the article.

Conflicts of Interest: The authors declare no conflict of interest.

References

[1]K. Eidmann, R. Sigel, Second-Harmonic Generation in an Inhomogeneous Laser-Produced Plasma, Phys. Rev. Lett., 34, 1975, 799--802

[2]Fujimoto, T. *Plasma Spectroscopy*; Clarendon Press: Oxford, GB, 2004

[3]EL Sherbini, A.M.; EL Sherbini, Th.M.; Hegazy, H.; Cristoforetti, G.; Legnaioli, S.; Palleschi, V.; Pardini, L.; Salvetti, A.; Tognoni, E. Evaluation of self-absorption coefficients of aluminum emission lines in laser-induced breakdown spectroscopy measurements. *Spectrochim. Acta Part B: At. Spectrosc.* **2005**, *60*, 1573 – 1579

[4]Parigger, C.G; Surmick, D.M.; G. Gautam, G.; EL Sherbini, A.M. Hydrogen alpha laser ablation plasma diagnostic. *Opt. Lett.* **2015**, *40*, 3436 – 3439.

[5]Parigger, C.G.; Surmick, D.M.; Gautam, G. Self-absorption characteristics of measured laser-induced line shapes. *J. Phys.: Conf. Ser.* **2017**, *810*, 012012.

[6]Irons, F.E. The escape factor in plasma spectroscopy—I. The escape factor defined and evaluated. *J. Quant. Spectrosc. Radiat. Transfer* **1979**, *22*, 1 – 20.

[7]Holstein, T. Imprisonment of Resonance Radiation in Gases. *Phys. Rev.* **1947**, *72*, 1212 – 1232.

[8]Holstein, T. Imprisonment of Resonance Radiation in Gases. II. *Phys. Rev.* **1951**, *83*, 1159 – 1168.

[9]Cowan, R.D.; Dieke, G.H. Self-Absorption of Spectrum Lines. *Rev. Mod. Phys.* **1948**, *20*, 418 – 455.

[10]Kielkopf, J.F.; Allard, N.F. Shift and width of the Balmer series Hα line at high electron density in a laser-produced plasma. *J. Phys B: At. Mol. Opt. Phys.* **2014**, *47*, 155701.

[11]Moon, H.-Y.; Herrera, K.K; Omenetto, N.; Smith, B.W.; Winefordner, J.D. On the usefulness of a duplicating mirror to evaluate self-absorption effects in laser induced breakdown spectroscopy, *Spectrochim. Acta Part B: At. Spectrosc.* **2009**, *64*, 702 – 713.

[12]EL Sherbini, A.M.; Parigger, C.G. Wavelength dependency and threshold measurements for nanoparticle-enhanced laser-induced breakdown spectroscopy. *Spectrochim. Acta Part B: At. Spectrosc.* 2016, *116*, 8 – 15.

[13]Ashraf M. EL Sherbini a, Christian G. Parigger b, Nano-material size dependent laser-plasma thresholds, Spectrochimica Acta Part B 124 (2016) 79–81

[14]A. M. El sherbini *et al* Plasma ignition threshold disparity between silver nanoparticle-based target and bulk silver target at different laser wavelengths 2019 *Plasma Sci. Technol.* 21 015502